Measurement of Model Inter-digital H Type Linac

T. Fukushima, T. Hattori, T. Hori,
K. Sato, E. Tojyo and K. Yoshida

Institute for Nuclear Study, University of Tokyo
Tanashi, Tokyo 188, Japan

Introduction

It is known that the inter-digital H type linac (IH linac) will have high shunt impedance per unit length (Z_S) for the acceleration of low velocity particles.[1-3] IH linac is therefore suitable for heavy ion acceleration, and Z_S as high as 120 MΩ/m has been realized in the post accelerator of the Tandem Van de Graaf accelerator in Munich.[4] This extremely high Z_S, however, is due to low capacitance between the drift tubes which are not mounted with focusing element and are very small. The Z_S depends on the capacitance per unit length, C, as $C^{-3/2}$.[1] In case of IH linac which directly accelerates the particle from usual Cockcroft-Walton injector, the Z_S will be considerably lower than the one in Munich linac due to large capacitance between closely aligned drift tubes with focusing element. Z_S also depends on particle velocity to be accelerated, $\beta=\frac{v}{c}$, as β^{-2},[1] and it is interesting in what velocity region the IH linac has the advantage over Alvarez linac. When β is assigned, Z_S is regulated by tank component dimensions such as waveguide ridge, drift tube, drift tube stem and so on. This will be examined by model tank experiment more efficiently than by the computational means because the electromagnetic field in the tank is not symmetric and is so much complicated. We are performing the rf measurement on a 1/6 scale model tank following the study on a simplified 1/8 scale model.[5] The aim of series of measurements are a) to obtain the dependence of the shunt impedance on the tank structure, b) to know the resonance characteristics for the various tank structure, which is necessary for equivalent circuit analysis, and c) to study the electric field distribution along the tank axis and to clarify the effect of the tank end structure on the field pattern.

Model Tank

The model tank in the present work is shown in Fig.1 and 2. It has been prepared by reducing to

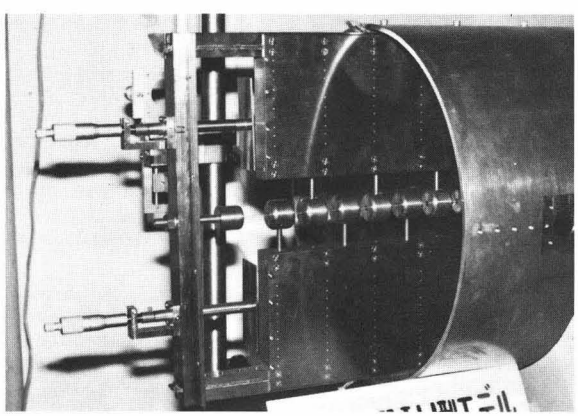

Fig.1 Picture of model tank.

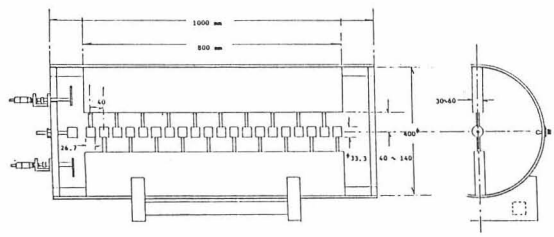

Fig.2 Composition of model tank.

a scale of one-sixth of the natural tank which will have a diameter of 2.4 m and will be operated by an rf of 25 MHz. The dimensions of the tank component which will affect the shunt impedance can be modified stepwise. These parameters are shown in Table 1.

Drift tubes are uniformly arranged to correspond a certain particle velocity β, β being 3, 4, 5 and 8 %. Most measurements are made on uniform drift tube arrangement, but the drift tube combinations corresponding to growing particle velocity are also examined.

The model is large enough to study the feature of the electromagnetic field in the tank. Since the rf contactors are employed in assembling the tank component, the experimental shunt impedance measured on the model tank can be meaningful.

Tank diameter	(D)	400 mm
length*)	(L)	800 ∿ 960 mm
Ridge length	(ℓ)	800 mm
width	(W)	30, 50, 60 mm
aperture**)	(d)	80, 120, 160, 200, 240 mm
Drift tube diameter		18.7, 26.7, 30, 33.3 mm
stem diameter		6, 8, 10 mm
Gap to cell length ratio (g/ℓ_c)		1/3

*) Electric tank length is adjusted by sliding the end plates.
**) Ridge to ridge distance.

Table 1. Parameters of model tank.

Resonance Characteristics

In Fig.3, resonant frequency of fundamental mode TE_{111} is plotted against β. The resonant frequency is given by $1/2\pi\sqrt{LC}$, L and C being inductance and capacitance of the tank, respectively, and it increases as the drift tube spacing become distant, i.e., β become large due to the decrease of the capacitance. In the tank for actual acceleration, therefore, the local resonance frequency varies according to the curves in Fig.3

as the structure of the tank changes along the longitudinal direction. Fig.3 inversely indicates

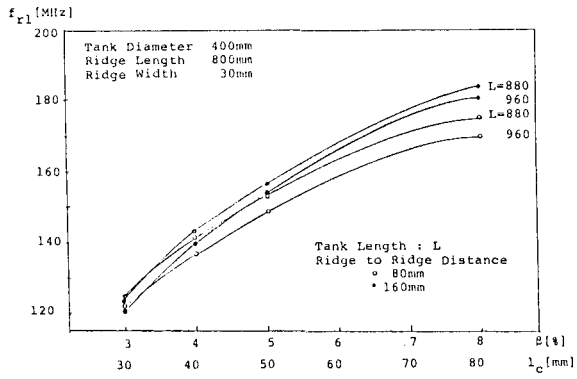

Fig.3 Frequency of fundamental mode.

the amount of frequency difference to be adjusted when one needs constant resonant frequency along the entire tank length. The frequency difference is 4 ∿ 13 % for 1 % change in β. It is also seen in Fig.3 that the resonant frequency increases when ridge to ridge distance is decreased in the β region above 4 % and vice versa around 3 %. This means that the growth of the capacitance is overcompensated by the fall of inductance due to the reduction of the effective cross section of the tank in the β region above 4 %.

Fig.4 and 5 are dispersion curves. As seen in the figures, the group velocity of the electromagnetic wave is definitely positive, periodic nature of the waveguide being not apparent in dispersion characteristics. One can determine the equivalent circuit parameters by using the accurately measured frequencies up to fourth harmonics. Analysis is now in progress.

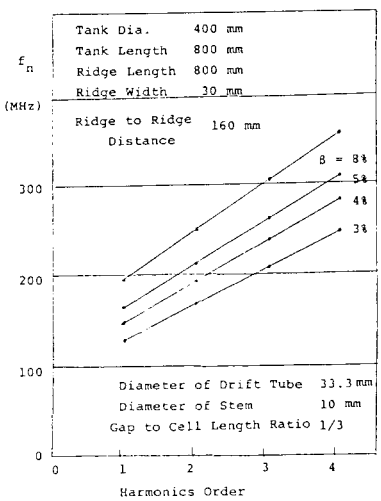

Fig.4 Dispersion curves (1).

It is seen in Fig.5 that the extension of ridge width causes the increases of resonant frequency, showing that the industance change rather than capacitance variation is again predominant at least around β = 4 %. It is also shown that the effect of the ridge structure on the fundamental mode is less than for higher mode.

Field Distribution

The electric field distribution was measured by the perturbing ball method with 6.6 ϕ × 30 mm and 5 ϕ × 30 mm cylinder of acrylic acid resin as a perturbator. Fig.6 shows the field distribution of typical constant velocity type tank of β = 4 %. In case of L = 800 mm i.e. ends of the ridge being shorted, the electric field strength is sinusoidal along the axis, as shown in Fig.6. This resonant mode is TE_{111}. In case of L = 880 and 960 mm, that is, for the resonator tank longer than the ridge, and having end spaces, the

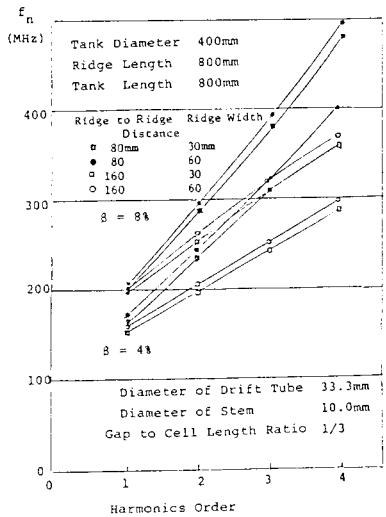

Fig.5 Dispersion curves (2).

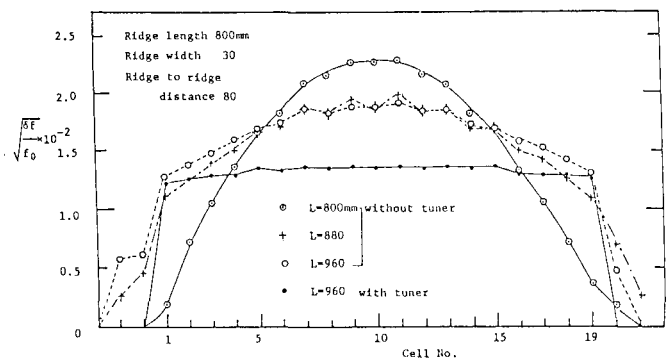

Fig.6 Electric field distribution along the axis (constant velocity model).

field distribution is fairly flat as shown in Fig.6. More flat field distribution is possible by using the capacitive tuners of brass plate (40 mm × 10 mm × 2 mm) as shown in Fig.1. Introduction of the capacitive tuner, however, results in 30 % reduction of Q-value. Therefore, two inductive tuners for tank end and eight inductive tuners for the ridge end are now being manufactured. We expect that the field distribution can be controlled by the inductive tuners without deteriolation of shunt impedance.

The gap-voltage distribution of the acceleration type tank was measured for various resonator lengths as shown in Fig.7. In case of L = 800 mm, the gap voltage distribution can be calculated by using the dispersion curves of constant velocity type tank (Fig.3) with the same dimensions. The calculated values agree with the measured values very well as shown in Fig.7. Therefore, the field distribution of acceleration-type tank which are shorted at the end of ridge, can be calculated by the dispersion curves for the constant velocity type model.

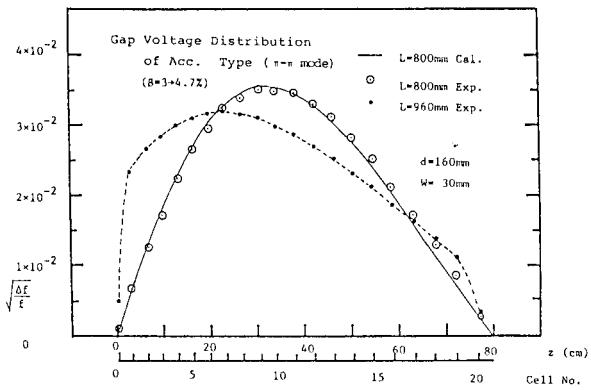

Fig.7 Gap voltage distribution along the axis (acceleration type model).

Shunt Impedance

Shunt impedance is obtained by measuring a Q-value and a resonant frequency shift $\Delta f/f_o$ due to a dielectric perturbator and by using the following equation,

$$Z_S = Q_o \frac{\Delta f}{f_o^2} \frac{L_C}{L_t} \alpha \frac{1.14}{r^2(\varepsilon-1)} \times 10^4 \left[\frac{M\Omega}{m}\right] ,$$

where Q_o is unloaded Q-value of the tank, L_t is tank length, L_C is total cell length, α is gap to cell length ratio g/ℓ_C, r is the radius of the dielectric rod spanned over entire tank through beam bore and ε is a dielectric constant of the rod.

The results are shown in Fig.8 and 9. The indicated shunt impedance is for model tank which is made of brass, and the value for the actual tank is $\sqrt{(\sigma_c/\sigma_b \cdot n)}$ times the one for the model, where σ_c, σ_b and n are the conductivity of the copper and of the brass, and the scaling factor, respectively. It is seen from Fig.8 that Z_S varies with β as nearly $\beta^{-1.4}$.

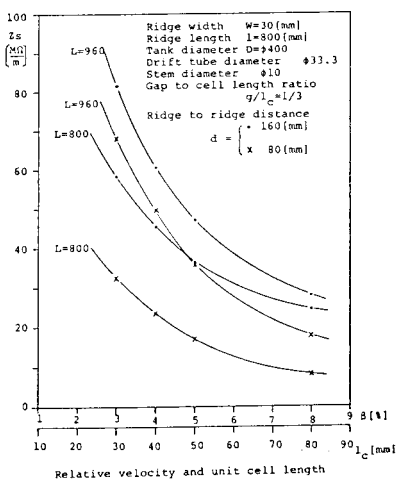

Fig.8 Dependence of shunt impedance on β.

In both figures, the effect of the tank end space on Z_S is clear. Since the ridge length is kept to be 800 mm, the model tank with L = 800 mm has no space at tank ends, whereas L = 960 mm means that 20 % of the tank is free cylindrical waveguide at its ends. The shunt impedance is remarkably higher for the model with the end space than for the one without the end space. It is supposed that the power loss increases unless the space for the longitudinal H field to turn at the tank ends is prepared. Shunt impedance for the tank with L = 880 mm, which is not shown in the figure, almost coincides with the one with L = 960 mm. This means that the preparation of end space causes the extension of the tank length, but the improvement of the field strength contributes for Z_S to be nearly constant. Thus the structure of the tank end is of great importance for improving the shunt impedance as well as for controlling the field distribution along the axis as described in the preceding section. An empty waveguide at the tank ends is the most simple example.

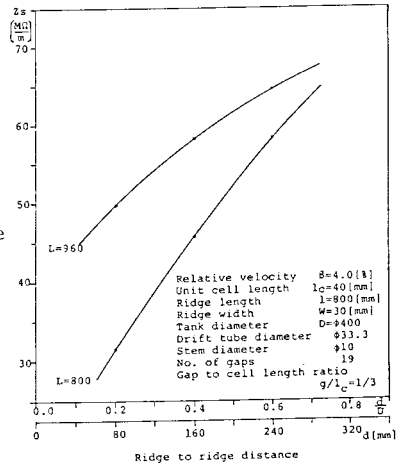

Fig.9 Dependence of shunt impedance on ridge to ridge distance.

Fig.9 shows the dependence of Z_S on a ridge to ridge distance. A larger distance is better as far as Z_S is concerned. This result has great significance and should be discussed further. On the other hand, a larger ridge to ridge distance results in a higher resonant frequency at a higher β as shown in Fig.3. If one wants to keep the resonant frequency of the tank at a given value under condition of the reasonable tank diameter, one has to use a ridge for the tank. We might conclude tentatively that the ridge dimension is determined from compromising the reasonable tank diameter and a shunt impedance at a given frequency.

Acknowledgment

The authors would like to thank Kitano Seiki Corporation and staffs of machine shop of INS for manufacturing the model resonator tank.

References

1) J. Pottier: IEEE Trans. Nucl. Sci., NS-16, No.3, 377 (1969)
2) E. Nolte et al: IEEE Trans. Nucl. Sci., NS-26, No.3, 3724 (1979)
3) P. M. Zeidlits and V. A. Yamnitskii: Plasma Phys., 4, 121 (1962)
4) E. Nolte et al: Nucl. Instrum. Meth. 158, 311 (1979)
5) N. Ueda et al; IEEE Trans. Nucl. Sci., NS-28, No.3, 3023 (1981)
6) W. Chahid: L'Onde Electrique, 11, 359, 171 (1957).